Neuron, Volume *92*

Supplemental Information

A Sensor for Low Environmental Oxygen in the Mouse Main Olfactory Epithelium

Katherin Bleymehl, Anabel Pérez-Gómez, Masayo Omura, Ana Moreno-Pérez, David Macías, Zhaodai Bai, Randall S. Johnson, Trese Leinders-Zufall, Frank Zufall, and Peter Mombaerts

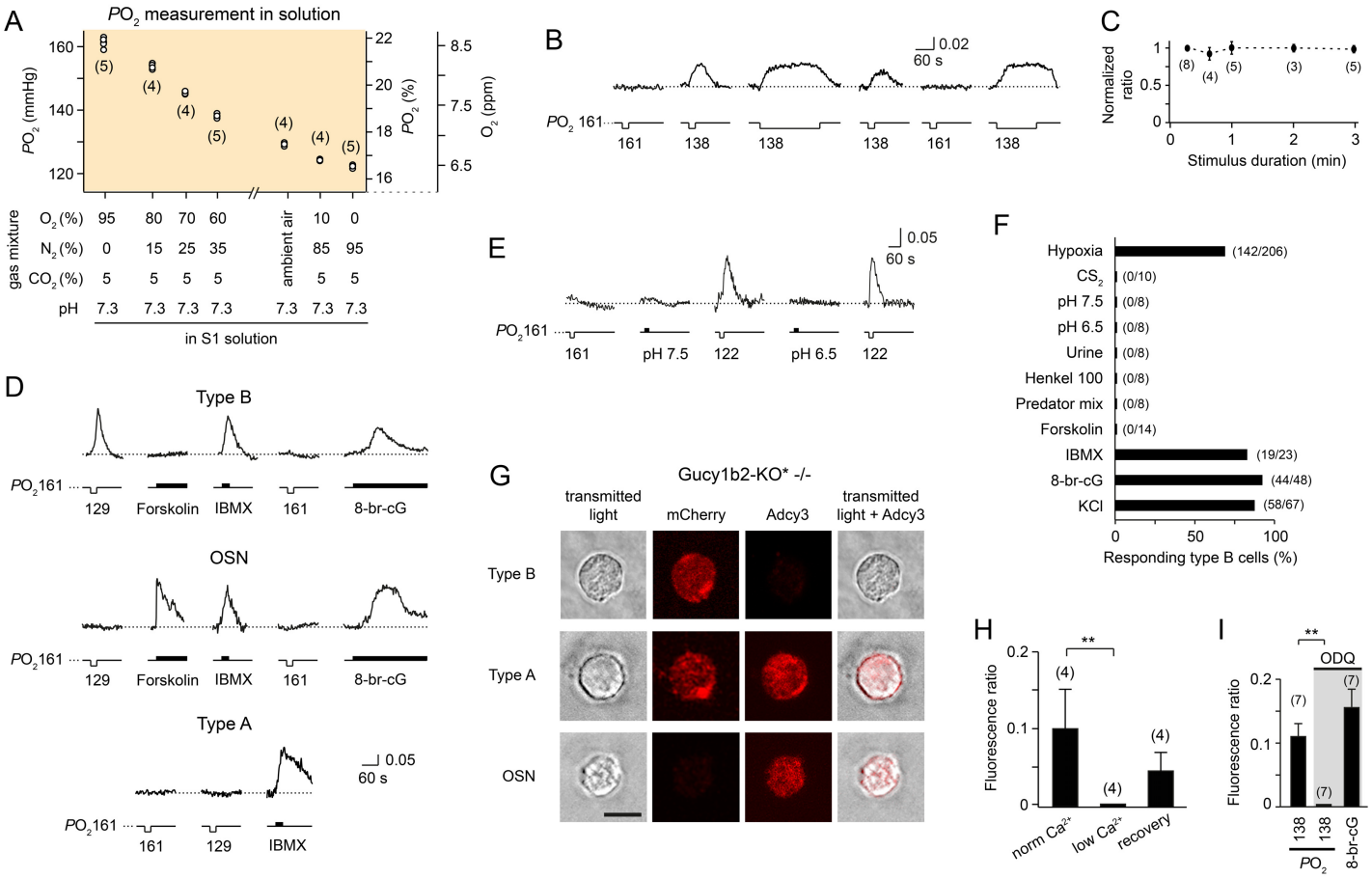
A
PO2 measurement in solution
PO2 (mmHg)
PO2 (%)
O2 (ppm)
gas mixture
O2 (%)
N2 (%)
CO2 (%)
pH
ambient air
in S1 solution
B
0.02
60 s
PO2 161
C
Normalized ratio
Stimulus duration (min)
D
Type B
OSN
Type A
Forskolin
IBMX
8-br-cG
E
0.05
60 s
pH 7.5
pH 6.5
F
Hypoxia
CS2
pH 7.5
pH 6.5
Urine
Henkel 100
Predator mix
Forskolin
IBMX
8-br-cG
KCl
Responding type B cells (%)
G
Gucy1b2-KO* -/-
transmitted light
mCherry
Adcy3
transmitted light + Adcy3
H
Fluorescence ratio
norm Ca2+
low Ca2+
recovery
I
ODQ
PO2
8-br-cG

Figure S1

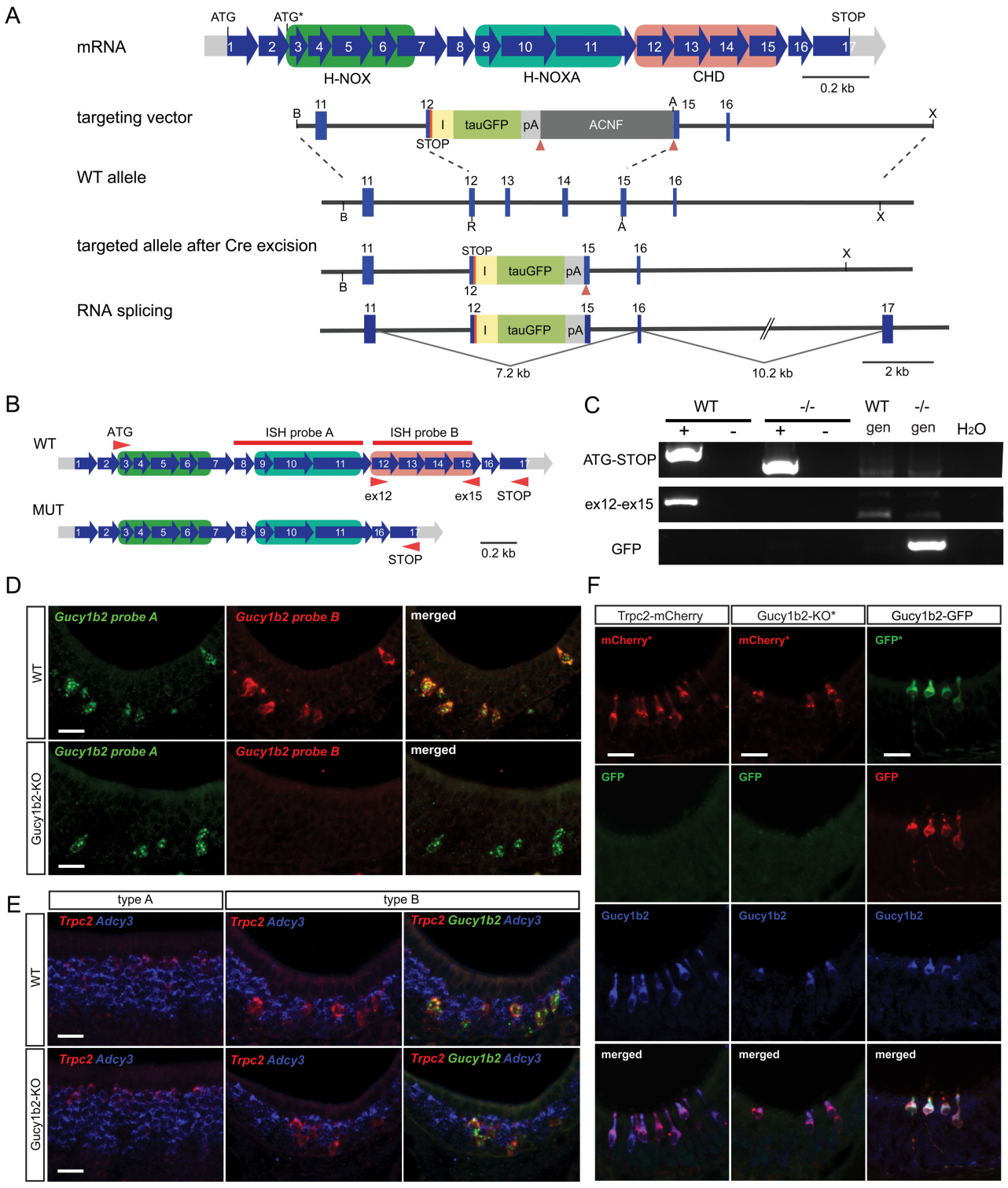
A
mRNA
ATG
ATG*
STOP
H-NOX
H-NOXA
CHD
0.2 kb
targeting vector
tauGFP
pA
ACNF
STOP
WT allele
targeted allele after Cre excision
RNA splicing
7.2 kb
10.2 kb
2 kb
B
WT
MUT
ATG
ISH probe A
ISH probe B
ex12
ex15
STOP
0.2 kb
C
WT
-/-
gen
H2O
ATG-STOP
ex12-ex15
GFP
D
Gucy1b2 probe A
Gucy1b2 probe B
merged
Gucy1b2-KO
E
type A
type B
Trpc2 Adcy3
Trpc2 Gucy1b2 Adcy3
F
Trpc2-mCherry
Gucy1b2-KO*
Gucy1b2-GFP
mCherry*
GFP*
GFP
Gucy1b2
merged

Figure S2

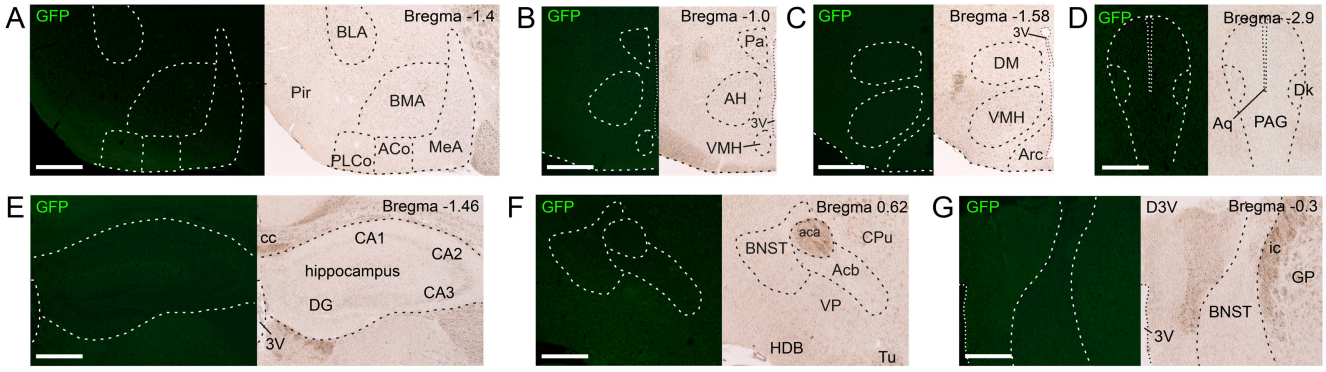
A
GFP
Bregma -1.4
BLA
Pir
BMA
PLCo
ACo
MeA
B
GFP
Bregma -1.0
Pa
AH
3V
VMH
C
GFP
Bregma -1.58
3V
DM
VMH
Arc
D
GFP
Bregma -2.9
Dk
Aq
PAG
E
GFP
Bregma -1.46
cc
CA1
CA2
hippocampus
CA3
DG
3V
F
GFP
Bregma 0.62
aca
CPu
BNST
Acb
VP
HDB
Tu
G
GFP
D3V
Bregma -0.3
ic
GP
BNST
3V

Figure S3

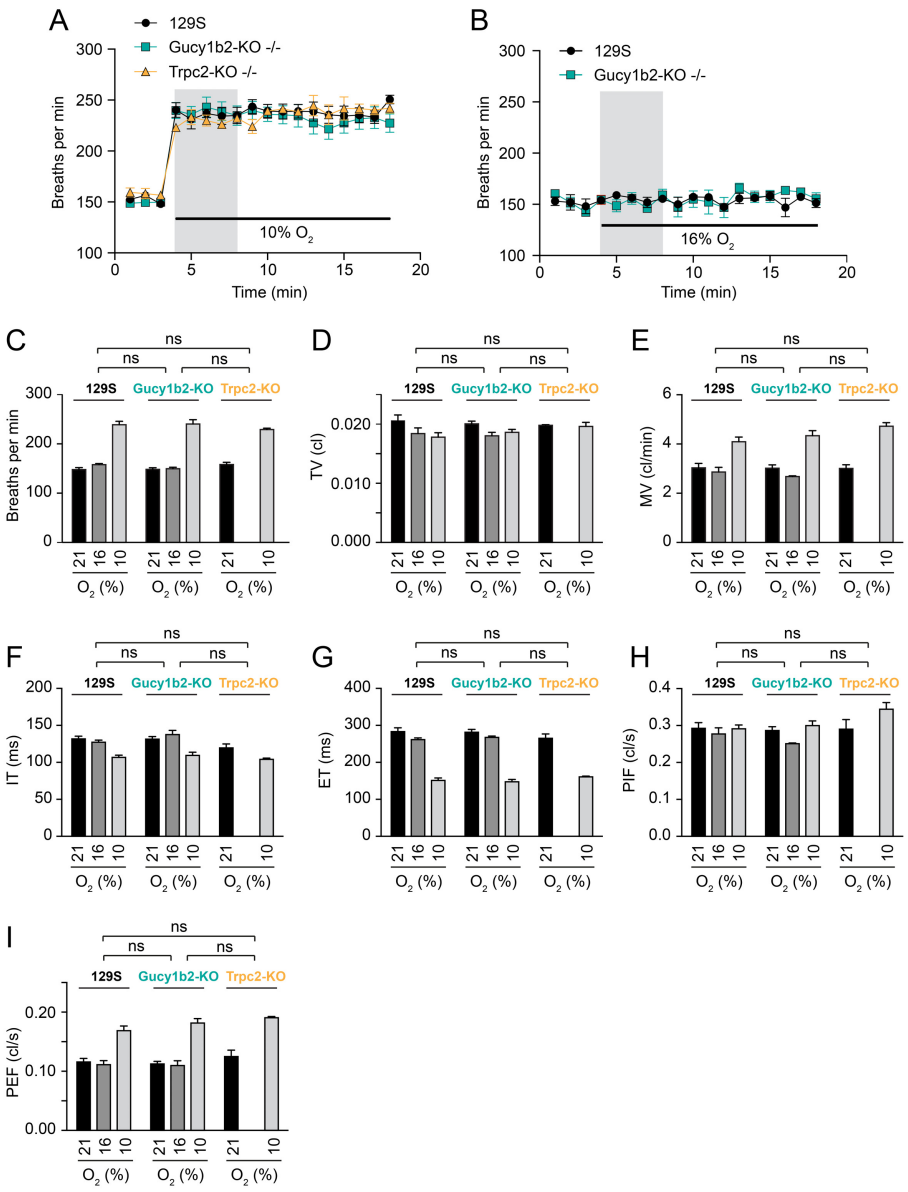
A
129S
Gucy1b2-KO -/-
Trpc2-KO -/-
Breaths per min
Time (min)
10% O2
B
129S
Gucy1b2-KO -/-
Breaths per min
Time (min)
16% O2
C
Breaths per min
D
TV (cl)
E
MV (cl/min)
F
IT (ms)
G
ET (ms)
H
PIF (cl/s)
I
PEF (cl/s)
ns
129S
Gucy1b2-KO
Trpc2-KO
O2 (%)

Figure S4

Figure S1, related to Figure 1.

Properties and Selectivity of Type B Cell Ca^{2+} Responses.

(A) Plot of the oxygen levels measured in extracellular solutions. Various gas mixtures as indicated were bubbled until saturation into S1 solution, keeping the CO_2 concentration and pH constant. Ambient air refers to a solution that was equilibrated in ambient air for at least 2 h at room temperature. Values were measured in ppm or % and converted into PO_2 (mmHg). Dissolved oxygen values were corrected for salinity of the solution. The number of independent measurements obtained on different days is indicated.

(B) Recording example indicating repeatability and effect of stimulus duration on Ca^{2+} responses to low oxygen. Responses were time-locked and there was no evidence for adaptation-like desensitization even after minute-long stimulation.

(C) Peak amplitude of Ca^{2+} responses to low oxygen was independent within the indicated range of stimulus durations. The number of independent recordings is indicated in the graph.

(D) Comparison of response properties of type B cells, canonical OSNs, and type A cells to various stimuli. Type B cells (n = 206) failed to respond to forskolin (50 µM), consistent with their lack of Adcy3 expression. Canonical OSNs (n = 85), which express Adcy3, responded to forskolin but not to low oxygen. Type A cells (n = 10) failed to respond to low oxygen, but responded to IBMX.

(E) Solutions with altered H^+ concentration (pH 7.5 or 6.5) failed to induce a Ca^{2+} response in type B cells.

(F) Summary plot indicating the discrimination capabilities of type B cells and demonstrating that these neurons do not respond to carbon disulfide (CS_2, 13 μM); diluted mouse urine (1:100); a mixture of 100 odorants (Henkel 100, diluted 1:100); and a mixture of several predator odors (see Materials and Methods for details). Results are based on recordings from 42 Gucy1b2-GFP -/- mice. The number of responding versus total cells tested is indicated above each bar.

(G) Examples of posthoc immunostaining of cells from Gucy1b2-KO* -/- mice enabling discrimination among type B cells (mCherry+, Adcy3-), type A cells (mCherry+, Adcy3+), and canonical OSNs (mCherry-, Adcy3+). Scale bar, 10 μm.

(H) Effect of external Ca^{2+} removal on low oxygen responses (122 mm Hg) analyzed in type B cells of Gucy1b2-GFP -/- mice (ANOVA: $F(2, 11) = 10.131$, $p < 0.005$; LSD: ** $p < 0.001$). Partial recovery was evident after restoring external Ca^{2+} concentrations to normal values (LSD: $p = 0.067$). The number of independent recordings is indicated above each bar.

(I) Group data showing type B cell Ca^{2+} responses from Gucy1b2-GFP -/- mice. Treatment with ODQ (10 μM) eliminates the response to low oxygen (138 mmHg) but not to 8-br-cGMP (500 μM).

Results are presented as mean ± SEM.

Figure S2, related to Figure 2.

The Gene-targeted Gucy1b2-D-IRES-tauGFP Mouse Strain.

(A) Targeting scheme of the Gucy1b2-D-IRES-tauGFP mutation. The *Gucy1b2* gene is located on chromosome 14, and consists of 17 coding exons. Functional domains of soluble guanylate cyclases are heme domains H-NOX and H-NOXA, and the cyclase homology domain CHD. The ATG* in the genomic DNA and in the mRNA depicts an alternative *ATG* site in the *Gucy1b2* transcripts identified in RNA extracted from whole olfactory mucosa. A deletion of the catalytic domain CHD of the *Gucy1b2* gene was generated by gene targeting in ES cells. The STOP codon *TGA* was inserted after the *EcoRI* site in exon 12. A segment of 4.3 kb of DNA comprising exon 12 to exon 15, encoding the cyclase homology domain of the Gucy1b2 enzyme, was replaced with an *IRES-tauGFP-pA-ACNF* cassette. The *ACNF* cassette was auto-excised during transmission through the male germline, leaving a single *loxP* site (pink triangle) behind in the genome, and resulting in the Gucy1b2-KO mutation. The exon-intron structure of the major transcript of *Gucy1b2* isolated from whole olfactory mucosa of homozygous Gucy1b2-KO -/- mice (MUT) was analyzed by 3'RACE with primers on exon 11 of *Gucy1b2*. Blue boxes represent exons. A segment of 7.2 kb after exon 11 including the entire *IRES-tauGFP-pA* cassette is spliced out, such that exon 11 is joined to exon 16 in the major transcript of *Gucy1b2* from Gucy1b2-KO mice. As a result, cells that express this mutant allele do not express GFP.

(B) Schematic diagram of the mRNA structure of *Gucy1b2* from wild-type (WT) and mutant (MUT) alleles. The positions of primers used for RT-PCR and riboprobes for ISH are indicated with red arrows and red bars respectively. ISH probe A detects exon 8 to exon 11, a common

region of the WT and MUT transcripts. ISH probe B detects exon 12 to exon 15, a segment that is deleted in MUT transcripts.

(C) RT-PCR analysis of the whole olfactory mucosa of wild-type (WT) and homozygous Gucy1b2-KO -/- mice at 7 weeks with three sets of primers (ATG to STOP, exon 12 to exon 15, and GFP). With the ATG-STOP primer set, a 1.6 kb PCR product was amplified from -/- cDNA compared to the 2.2 kb PCR product from WT. No PCR product was detected from -/- cDNA with the set of primers for exon 12 and exon 15. There is no *GFP* amplifiable from -/- cDNA due to splicing of the whole IRES-tauGFP-pA cassette in *Gucy1b2* transcripts. + , RT+; -, RT-; WT gen, genomic DNA of WT tail; -/- gen, genomic DNA of -/- tail.

(D) In situ hybridization for *Gucy1b2* on coronal sections of the MOE of a wild-type 129S6/SvEvTac mouse and a Gucy1b2-KO -/- mouse (backcrossed 11 times to 129S6/SvEvTac) at 3 weeks. Scale bar, 20 μm.

(E) In situ hybridization for *Trpc2* on coronal sections of the MOE of a wild-type 129S6/SvEvTac mouse and a Gucy1b2-KO -/- mouse (backcrossed 11 times to 129S6/SvEvTac) at 3 weeks. Type A cells express, in addition to *Trpc2*, also *Adcy3* but not *Gucy1b2*. Conversely type B cells express, in addition to *Trpc2*, also *Gucy1b2* but not *Adcy3*. Scale bar, 20 μm.

(F) Immunohistochemistry for GFP and Gucy1b2 of a coronal section of the MOE of a Trpc2-IRES-taumCherry -/- mouse at 10 weeks; a mouse that is Gucy1b2-KO -/- and Trpc2-IRES-taumCherry -/- (Gucy1b2-KO*) at 10 weeks; and a Gucy1b2-GFP -/- mouse at 8 weeks. Type B

cells are Gucy1b2 immunoreactive but immunonegative for GFP due to splicing of the mutant transcripts. Truncated Gucy1b2 protein is expressed in type B cells. The antigen region of the Gucy1b2 antibody (654-675 in the Gucy1b2 sequence) is partially intact in the truncated Gucy1b2 protein in the mutant mouse: it contains 13 amino acids of the 22 amino acids that constitute the antigen region. The Gucy1b2 antibody gives a weaker signal in Gucy1b2-KO -/- mice. The GFP antibody gives a signal (red) in the Gucy1b2-GFP -/- mouse. GFP* and mCherry* show the intrinsic fluorescence of GFP and mCherry. Scale bar, 20 μm.

Figure S3, related to Figure 4.

Absence of GFP Expression in Selected Brain Regions of Gucy1b2-GFP -/- Mice.

Visualization of intrinsic GFP fluorescence (green) in coronal brain sections from Gucy1b2-GFP -/- mice failed to identify labeled cells in amygdala and piriform (Pir) cortex (A), hypothalamus (B, C), periaqueductal grey (PAG; D), hippocampus (E), nucleus accumbens (Acb; F), and bed nucleus of the stria terminalis (BNST; F, G). Transmitted light images (right panels) aid in identifying the various regions as indicated. 3V, third ventricle; ACo, anterior cortical amygdaloid nucleus; AH, anterior hypothalamic area; Aq, aqueduct; BLA, basolateral amygdaloid nucleus; BMA, basomedial amygdaloid nucleus; CA1-3, hippocampus field CA1-3, respectively; cc, corpus callosum; CPu, caudate putamen; D3V, dorsal third ventricle; DG, dentate gyrus; Dk, nucleus of Darkschewitsch; DM, dorsomedial hypothalamic nucleus; fr, fasciculus retroflexus; GP, globus pallidus; HDB, nucleus of the horizontal limb of the diagonal band; ic, internal capsule; MeA, medial amygdaloid nucleus; Pa, paraventricular hypothalamic nucleus; PLCo, posterolateral cortical amygdaloid nucleus; Tu, olfactory tubercle; VMH, ventromedial hypothalamus; VP, ventral pallidum. Scale bar, 400 μm. Distance to bregma zero coordinate is indicated in mm.

Figure S4, related to Figure 4.

Whole-body Plethysmography Reveals Normal Ventilatory Responses to Hypoxia in Gucy1b2-KO -/- Mice and in Trpc2-KO -/- Mice.

(A) Hypoxic ventilatory response of wild-type 129S (129S6/SvEvTac), Gucy1b2-KO -/- (129S6/SvEvTac background) and Trpc2 KO -/- mice (129S6/SvEvTac background) exposed to 10% O_2 for 15 min; n = 9 (129S), n = 10 (Gucy1b2-KO -/-), n = 3 (Trpc2-KO -/-).

(B) Time course illustrating the absence of hyperventilatory response in 129S and Gucy1b2-KO -/- mice exposed to 16% O_2 for 15 min; n = 4 (129S), n = 4 (Gucy1b2-KO -/-).

(C-I) Average respiratory parameters recorded during the first 5 min at 10% O_2 (grey box in (A)) or 16% O_2 (grey box in (B)). There were no significant differences in ventilatory responses to hypoxia between the three genotypes in any of the measured parameters (ANOVA: $F(3,43)$ = 0.713 - 2.208, p = 0.12 - 0.55; ns = non-significant). Tidal volume (TV), minute volume (MV), inspiration time (IT), expiration time (ET), peak inspiratory flow (PIF), peak expiratory flow (PEF); n = 9 (129S), n = 10 (Gucy1b2-KO -/-), n = 3 (Trpc2-KO -/-) for 10% O_2 and n = 4 (129S), n = 4 (Gucy1b2-KO -/-) for 16% O_2 exposures.

Results are presented as mean ± SEM.

SUPPLEMENTAL EXPERIMENTAL PROCEDURES

Mice

Adult (6-23 weeks old) mice (either sex) were kept under standard light/dark cycle (12:12; lights on 0600; lights off 1800) or reverse light/dark cycle (behavioral experiments; 12:12; lights off 0700; lights on 1900) with food and water *ad libitum*. The following strains were used: B6;129P2-*Gucy1b2<tm3Mom>*/MomJ (Stock# 021063; Gucy1b2-IRES-tauGFP, referred to as Gucy1b2-GFP; RRID:IMSR_JAX:021063) (Omura and Mombaerts, 2015); B6;129P2-*Trpc2<tm2Mom>*/MomJ (Stock# 006733; Trpc2-IRES-taumCherry; RRID:IMSR_JAX:006733) (Omura and Mombaerts, 2014); 129S6.129P2-*Trpc2<tm1Mom>*/MomJ (Stock# 007890; Trpc2-KO; RRID:IMSR_JAX:007890) (Omura and Mombaerts, 2014); B6;129P2-*Cnga2<tm1Mom>*/MomJ (Stock# 006644; Cnga2-KO; RRID:IMSR_JAX:006644) (Zheng et al., 2000); B6;129P2-*Gucy1b2<tm2Mom>*/MomJ (Stock# 017517; Gucy1b2-D-IRES-tauGFP, referred to as Gucy1b2-KO; RRID:IMSR_JAX:017517); and 129S6.129P2(B6)-*Gucy1b2<tm2Mom>*/MomJ (Stock# 021844; Gucy1b2-KO backcrossed 10 times to 129S6/SvEvTac; RRID:IMSR_JAX:021844). These strains are publicly available from The Jackson Laboratory. Crossing mice with individual gene-targeted mutations yielded mice that are heterozygous or homozygous for Gucy1b2-KO and homozygous for Trpc2-IRES-taumCherry (referred to as Gucy1b2-KO* +/- or -/-); homozygous for Trpc2 and homozygous for Gucy1b2-GFP (Trpc2-KO* -/-); and hemizygous or homozygous for Cnga2-KO and homozygous for Trpc2-IRES-taumCherry (Cnga2-KO* MUT). Mice carrying the Trpc2-KO mutation and used for whole-body plethysmography were backcrossed 8 times to 129S6/SvEvTac. Mice carrying

only the Gucy1b2-KO mutation were backcrossed 11 times to 129S6/SvEvTac. Mice carrying the Gucy1b2-IRES-tauGFP mutation and all crosses were in a mixed 129 x C57BL/6 background.

Animal care and experimental procedures were performed in accordance with the guidelines established by the German Animal Welfare Act, European Communities Council Directive 2010/63/EU, the institutional ethical and animal welfare guidelines of the Max Planck Institute of Biophysics and the Max Planck Research Unit for Neurogenetics (approval came from the Veterinäramt of the City of Frankfurt), the Saarland University (approval number of the Institutional Animal Care and Use Committee: H-2.2.4.1.1), and the UK Home Office and University of Cambridge. The number of animals used is a minimum necessary to provide adequate data to test the hypotheses of this project. We have minimized the number of animals required by the animal welfare committees wherever possible.

En face imaging of GFP+ neurons in the MOE

Gucy1b2-GFP -/- mice (6 weeks to 14 months old) were used. Mice were anesthetized by injection of ketamine HCl and xylazine (210 mg/kg and 10 mg/kg body weight) and decapitated. The MOE was peeled off from the lateral turbinate, and transferred into Ringer's solution (140 mM NaCl, 5 mM KCl, 1 mM $CaCl_2$, 1 mM $MgCl_2$, 10 mM Hepes, 10 mM glucose, 1 mM Na pyruvate, pH 7.4). The MOE sample was flattened by trimming, transferred to a tissue slice chamber (Warner instruments) with the cilia layer facing up, and fixed with a stainless steel slide anchor. En face view images of the GFP+ neurons were collected with a Zeiss LSM710 confocal

microscope (Axio Imager Z1) equipped with an Achroplan 100x/1.00 water-immersion objective (Zeiss).

Calcium imaging

For Ca^{2+} imaging experiments, mice (6-23 weeks old) were decapitated following anaesthesia. Cells were freshly dissociated from the MOE without the use of enzymes during the dissociation procedure. The turbinates were dissected carefully out of the nasal cavity and minced in low Ca^{2+}-solution containing (in mM): 120 NaCl, 25 $NaHCO_3$, 5 KCl, 4.25 $CaCl_2$, 5 EGTA, 1 $MgCl_2$, 5 BES, pH = 7.3, 300 mOsm. Minced tissue was incubated in this solution for an additional 15 min (37°C) and then gently passaged using a fire-polished Pasteur pipette and oxygenated solution S1 (95% O_2/ 5% CO_2; RT = 21°C) consisting of (in mM): 120 NaCl, 25 $NaHCO_3$, 5 KCI, 1 $MgSO_4$, 1 $CaCl_2$, 10 Glucose, 5 BES, pH 7.3, 300 mOsm. Dissociated cells were placed on coverslips previously coated with poly-L-lysine (0.01%) and laminin (0.1%) and incubated in oxygenated S1 solution containing the ratiometric Ca^{2+}-indicator fura-2/AM (6 µM, Invitrogen), 0.01% Pluronic-F127 (Invitrogen) and 0.67% DMSO for 30 min at RT. Coverslips containing fura-2 loaded cells were placed in a laminar flow recording chamber (RC-27, Warner Instruments) and continuously perfused with oxygenated S1 solution at a rate of ~ 10 µl/s (RT). Ca^{2+} imaging was performed using an upright microscope (Olympus BX-51WI) equipped with a 20x/1.00 water immersion objective (XLUMPlanFL N) and a CCD camera (ORCA-R2, Hamamatsu Photonics). Fura-2 ratios were determined at 340 and 380 nm. Image pairs were acquired at 0.5 Hz and analyzed using ImageJ (NIH) and Igor Pro software (Wavemetrics) as described (Pérez-Gómez et al., 2015; Schmid et al., 2010). Chemostimuli were prepared freshly

each day and diluted in oxygenated solution S1 giving the following final concentrations: Henkel 100 containing a mixture of 100 volatile odorants (1:100; Henkel) from several classes and groups such as aromatics, aliphatics, alcohols, aldehydes, esters, ethers, ketones, amines, alkanes, heterocyclics and others (Wetzel et al., 1999); urine from C57BL/6 male mice, 1:100; predator odor mix (2-PT, 2-propylthietane; TMT, 2,5-dihydro-2,4,5-trimethylthiazole; PEA, ß-phenylethylamine; 2,6-DMP, 2,6-dimethylpyrazine; each at 100 µM) (Pérez-Gómez et al., 2015); CS_2, 13 µM; forskolin, 50 µM; IBMX (3-isobutyl-1-methylxanthine), 100 mM; 8-br-cGMP (8-bromoguanosine 3',5'-cyclic monophosphate), 500 µM; and KCl, 30 mM. Stimuli were bath-applied in random order. If not otherwise stated, stimulus duration was 20 s. For IBMX and KCl, we used 30-s stimuli; forskolin and 8-br-cGMP were applied for 2 min or sometimes longer. KT5823 (10 µM; CAS# 126643-37-6) and ODQ (1H-[1,2,4]oxadiazolo[4,3-a]quinoxalin-1-one; 10 µM; CAS# 41443-28-1) were obtained from Tocris. L-NAME (N_ω-nitro-L-arginine methyl ester hydrochloride) was obtained from Sigma. Cells were treated with these compounds for 10-15 min. ODQ (1H-[1,2,4]oxadiazolo[4,3-a]quinoxalin-1-one; CAS# 41443-28-1) was obtained from Tocris. Experiments with reduced external Ca^{2+} concentrations used oxygenated S1 solution buffered with 1 mM EGTA (ethylene glycol-bis(2-aminoethylether)-N,N,N′,N′-tetraacetic acid) and no added Ca^{2+}. Unless otherwise stated chemicals were purchased from Sigma.

Oxygen measurements and calibration

Oxygen levels were adjusted by bubbling S1 solution with gas mixtures until reaching saturation or by delivering a steady stream of gas mixtures to the behavioral chambers until reaching

equilibrium. Dissolved oxygen was measured with an oxygen electrode calibrated for temperature of the solution and atmospheric pressure (GMH3630, Greisinger electronic GmbH, Germany). Values were corrected for the salinity of the solutions (Rounds et al., 2013). S1 solution oxygenated with 95% O_2, 0% N_2, 5% CO_2 resulted in an average PO_2 of 161 mmHg. For the in vivo experiments, we used a dedicated gas detector (X-am 5000, Dräger, Germany) to measure actual O_2 and CO_2 levels in the environmental air of our behavioral chambers. Electrodes were calibrated before each measurement according to the manufacturer's instructions. PO_2 values in the figures refer to the mean value determined from independent measurements obtained on different days before an experiment.

Posthoc immunostaining of cells from Gucy1b2-KO* and Cnga2-KO* mice

To discriminate type B cells from type A cells in Gucy1b2-KO* and Cnga2-KO* mice, posthoc immunostaining was performed following Ca^{2+} imaging directly in the recording chamber (Chamero et al., 2011), in order to distinguish Trpc2+ Adcy3- (type B) cells versus Trpc2+ Adcy3+ (type A) cells. Dissociated cells were fixed using phosphate-buffered saline (PBS) containing 4% paraformaldehyde (PFA) for 10 min at RT, permeabilized and incubated for 10 min in blocking solution [4% horse serum, 1% bovine serum albumin fraction V (Roth), 0.3% Triton X-100 in PBS], incubated with rabbit anti-Adcy3 (1:1000, 1 h, room temperature, SC-588, Santa Cruz, RRID:AB_630839), and washed in blocking solution (5 min) followed by an incubation with secondary antibody (1:800, 30 min, room temperature, Alexa Fluor 633 goat anti-rabbit, Thermo Fisher Scientific, RRID:AB_2535731).

Generation of the Gucy1b2-D-IRES-tauGFP (Gucy1b2-KO) strain

To generate the targeting vector for the Gucy1b2-KO mutation, a 4.2 kb *BamHI-EcoRI* fragment containing exon 11 and part of exon 12 (left homology arm) and a 7.2 kb *AccIII–XhoI* fragment containing part of exon 15 to the intron between exon 16 and exon 17 (right homology arm) were isolated from bacterial artificial chromosome clone bMQ-312D1 (Source Bioscience). A *STOP-PacI-IRES-tauGFP-pA-ACNF-PacI* cassette was inserted between the arms. This design results in a deletion of a 4.3 kb segment of genomic DNA containing part of exon 12 to part of exon 15 and encoding the entire cyclase homology domain (CHD) of *Gucy1b2*. Embryonic stem cells from parental line E14 were electroporated with the linearized targeting vector. G418-resistant clones were screened by Southern blotting using a 5' external probe (nucleotides 62413377-62413847 from NC_000080.6, *AseI* digestion of genomic DNA) and a 3' external probe (nucleotides 62396184-62396756 from NC_000080.6, *DraI* digestion). Targeted ES clones were injected into C57BL/6J blastocysts, chimeras were bred with C57BL/6J mice, and a strain established from targeted ES cell clone 4-187 initially in a mixed 129 x C57BL/6 background. An inbred strain called Gucy1b2-D-IRES-tauGFP (129S6/SvEvTac-N11) was then generated by eleven backcrosses to 129S6/SvEvTac. Mice were maintained in specified pathogen-free conditions in individually ventilated cages of the Tecniplast green line.

RT-PCR

Total RNA was extracted from the lateral part of the whole olfactory mucosa of two Gucy1b2-KO -/- mice and two +/+ littermates in a mixed 129 x C57BL/6 background at 7 weeks with

TRIzol reagent (Thermo Fisher Scientific). DNaseI-treated total RNA was purified with RNAeasy columns (Qiagen) followed by clean up protocol. Purified total RNA was reverse-transcribed using Superscript III (Thermo Fisher Scientific) with oligo dT $_{(20)}$ primer (Thermo Fisher Scientific). For amplification of the *Gucy1b2* gene, two set of primers were used, ATG-STOP (ATG; *ATGTACGGATTTATCAACACCT*, STOP; *TCACAACACAGCACAGAAGGCA*) and ex12-ex15 (exon 12; *GAGAATTCGAGACGTGTACC*, exon 15; *CCTTCCCATCAGCGAGAGCTG*). To check GFP expression, PCR was performed with GFP-for; *GCATCAAGGTGAACTTCAAGATCCG* and GFP-rev; *AGCTCGTCCATGCCGAGAGTGATC*.

3'-Rapid amplification of cDNA end (3'-RACE) analysis

To investigate the transcript structure of *Gucy1b2* in the whole olfactory mucosa, 3'-RACE was performed using the SMARTer RACE cDNA amplification kit (Clonetech Laboratories) according to manufacturer's protocol. Briefly, total RNA was extracted from lateral whole olfactory mucosa of Gucy1b2-KO -/- and +/+ littermates in a mixed 129 x C57BL/6 background at 7 weeks, and was used as template for first strand cDNA synthesis. The 3'-RACE reactions were performed in two steps. First amplification was performed with RACE-ex10-11; *GCCAGCCGACACTCAAACTCCGGGGTC* and Universal Primer A Mix (Clontech Laboratories), then a nested reaction was performed with Nested Universal Primer A (Clontech Laboratories), and RACE-ex11-1; *CATCGCTCCCCACGACACGACCAGGG* or RACE-ex11-2; *CATGTGGCCAACCAGCTCAAGGAGGG*. Amplified PCR products were cloned into pGEM-T-easy vector (Promega) and sequences were analyzed.

In situ hybridization

Three-week old Gucy1b2-KO -/- mice and 129S6/SvEvTac wild-type mice were analyzed. Dissection, sample preparation, and ISH were performed as described (Ishii et al., 2004). ISH probe A was prepared from exon 8 to exon 11 of *Gucy1b2* (nucleotides 965-1673 from NM_172810.3), and ISH probe B was prepared from exon 12 to exon 15 (nucleotides 1719-2321 from NM_172810.3). The *Trpc2* and *Adcy3* riboprobes have been described (Omura and Mombaerts, 2014). Images were collected with a Zeiss LSM 710 confocal microscope.

Immunohistochemistry of the MOE

Immunohistochemistry was performed as described (Omura and Mombaerts, 2015). Mice were Trpc2-IRES-taumCherry -/- at 10 weeks; Trpc2-IRES-taumCherry -/- and Gucy1b2-KO -/- at 10 weeks; and Gucy1b2-GFP -/- at 8 weeks. The following primary antibodies were applied: rabbit anti-Gucy1b2 (1:500) (Omura and Mombaerts, 2015), and chicken anti-GFP (1:1000, GFP-1020, Aves Labs, RRID:AB_10000240). After one overnight incubation with primary antibodies at 4°C, sections were incubated at 1.5 h at room temperature with secondary antibodies: donkey anti-rabbit IgG-Alexa647 (1:500, 711-606-152, Jackson ImmunoResearch Laboratories, RRID:AB_2340625) for rabbit anti-Gucy1b2, donkey anti-chicken IgY-Alexa488 (1:2000, 703-545-155, Jackson ImmunoResearch Laboratories, RRID:AB_2340375) for chicken anti-GFP on the sections of Trpc2-IRES-taumCherry and donkey anti-chicken IgY-Rhodamine Red X (1:1000, 703-295-155, Jackson ImmunoResearch Laboratories, RRID:AB_2340371) for chicken

anti-GFP on the sections of Gucy1b2-GFP -/- mice. Sections were analyzed with a Zeiss LSM 710 confocal microscope.

Analysis of GFP expression in brain sections of Gucy1b2-GFP -/- mice

Gucy1b2-GFP -/- mice at 8 weeks (n = 3) were transcardially perfused with 4% PFA in PBS. Tissue was dissected, post-fixed for 2 h and equilibrated overnight in PBS containing 30% sucrose at 4°C. Brains were snap-frozen in a dry ice/2-methylbutane bath. Coronal sections (18 µm) were collected on a cryostat (Microm HM525) and mounted onto SuperFrost Plus glass slides. GFP fluorescence was visualized using both intrinsic GFP fluorescence and anti-GFP immunostaining. Both methods gave the same results. Immunohistochemical procedures were conducted at room temperature, with the exception of primary antibody incubations (4°C). The following primary and secondary antibodies were used: chicken anti-GFP (1:1000, ab13970, Abcam, RRID:AB_300798) and goat anti-chicken IgG-Alexa Fluor-555 (1:1000, A-21437, Life Tech, RRID:AB_2535858). All sections were counterstained with Hoechst 33342 (1:10000) and mounted with DAKO fluorescent mounting medium. Fluorescence images were acquired on an Olympus IX71 microscope. Anatomical limits of selected brain regions were outlined in all sections by superimposing nuclear counterstains onto transmitted light images and using a mouse brain atlas (Paxinos and Franklin, 2001). As key landmarks we used selected brain structures including hippocampus, optic tract, fornix, third ventricle, internal and external capsule, lateral ventricle, anterior and posterior commissure, olfactory tubercle, lateral olfactory tract, nucleus of Darkschewitsch, and piriform cortex.

Imaging c-Fos immunoreactivity in olfactory bulb neurons

Singly-housed mice kept in reverse light/dark cycle for at least one week were habituated to a behavioral chamber (26×17×21 cm Makrolon polycarbonate box with lid) for 3 days (30 min each day). The chamber contained an entry port for gas mixture delivery (standard control gas mixture: 20% O_2, 80% N_2; flow rate: 3 l/min) and an exhaust port. On day 4, mice were exposed first to a gas mixture containing 20% O_2 for 30 min and subsequently to either a low oxygen containing gas mixture (16% O_2, 84% N_2) or the 20% O_2 gas mixture for an additional 10 min. All training and testing procedures were monitored using video recording. After oxygen exposure mice were returned to their home cage for 90 min to enable c-Fos accumulation before anesthetizing (195 mg/kg body weight ketamine and 18 mg/kg body weight xylazine) and transcardially perfusing the mice with 4% PFA in PBS. Tissue was dissected, post-fixed for 2 h and equilibrated overnight in PBS containing 30% sucrose at 4°C. Olfactory bulbs were snap-frozen in a dry ice/2-methylbutane bath. Sagittal sections (18 µm) were collected on a cryostat (Microm HM525) and mounted onto SuperFrost Plus glass slides. Immunohistochemical procedures were conducted at room temperature, with the exception of primary antibody incubations (4°C). The following primary and secondary antibodies were used: for Gucy1b2-GFP -/- mice, goat polyclonal anti-c-Fos (1:200, sc-52-G, Santa Cruz Biotechnology, RRID: AB_2629503) and Alexa Fluor-546 donkey anti-goat (1:500, A-11056, Life Tech, RRID:AB_2534103); for Gucy1b2-KO* mice, rabbit anti-RFP (1:500, 600401379, Rockland, RRID:AB_2209751), goat polyclonal anti-c-Fos (1:200, sc-52-G, Santa Cruz Biotechnology, RRID: AB_2629503), Alexa Fluor-555 donkey anti-rabbit (1:500, A-31572, Life Tech, RRID:AB_162543) and Alexa Fluor-488 donkey anti-goat (1:500, A-11055, Life Tech,

RRID:AB_2534102). Sections were incubated with Hoechst 33342 (1:10,000) and mounted with DAKO fluorescent mounting medium. Through the nuclear staining, the boundaries of densely packed cells in the vicinity of a given GFP+ or mCherry+ glomerulus were defined and c-Fos immunoreactive cells within this area were counted (Pérez-Gómez et al., 2015). These cellular counts (mean number of nuclei/mm^3) were evaluated blindly for each mouse.

Conditioned place aversion

Experiments were conducted in a custom-made arena composed of two chambers of equal size (26×17×21 cm each; Makrolon polycarbonate box with lid) with a connecting opening (5 cm wide, 4 cm high). The opening could be closed by a sliding door to limit accessibility to only one chamber. Both chambers contained a port for gas mixture delivery (standard control gas mixture: 20% O_2, 80% N_2; low oxygen gas mixture: 16% O_2, 84% N_2; flow rate: 3l/min) and an exhaust port. A tube was affixed to the gas mixture delivery port outside each chamber. For each chamber, we used a separate, computerized QCAL gas mixing system (GMS_3CH, Oberostendorf, Germany) operated by dedicated software (version 4.3). The arena was surrounded by contextual cues (high-contrast geometric objects located on the walls surrounding the chambers). The conditioned place aversion protocol included preconditioning, conditioning, and testing phases. During preconditioning (performed across 3 days) all mice were allowed to explore the environment (both chambers) for 30 min per day. Following preconditioning, mice underwent conditioning for 3 days with alternating treatment-chamber pairings during the morning and afternoon. During the conditioning phase, mice were placed in the paired chamber without access to the other compartment. Each chamber was dedicated to contain either the gas

mixture (20% O_2, control chamber) or the low oxygen gas mixture (16% O_2, low-oxygen chamber). Half of the mice were placed into the control chamber in the morning, followed by placement in the low-oxygen chamber in the afternoon. The other half of the mice were treated in the reverse order. Morning and afternoon sessions were separated by ≥ 3 h. The position of the low-oxygen chamber was randomized across trials and mice, relative to the visual cues outside the arena. On the test day, mice were placed into the 16%-paired chamber and had access to both chambers (but both now at 20% O_2) for 10 min. Behavior was recorded and automatic tracking was performed by reducing the speed of the digital videos to 1 frame/s. After a thresholding step to 8-bit B/W (binary contrast enhancement), particles were 2D-analyzed using ImageJ (NIH) Mtrack2. A reduction of the time spent in a chamber associated with 20% or 16% O_2 exposure indicated aversion of the condition. Preference index was calculated as the difference between the time a given mouse spent in the low-oxygen chamber (t16) and the time the same mouse spent in the control chamber (t20) as follows: (t16 - t20)/(t16 + t20). For statistical analysis, a one-sample t test against 0.0 was used. Multiple groups were compared using a two-way analysis of variance (ANOVA) with the Fisher's least significant difference (LSD) as a posthoc comparison.

Morris water maze

Mice were 7-16 weeks old. A plastic circular pool (120 cm in diameter) filled with tepid water (23°C ± 1°; depth, 30 cm) was made opaque using non-toxic white paint (VBS Hobby Service GmbH, Germany). Trial starting points were marked outside the pool as north (N), south (S), east (E), and west (W), dividing the maze into four equal quadrants (NE, SE, SW, NW). A

circular transparent platform (diameter, 10 cm) was submerged to ~1 cm below the surface, and was kept in a fixed position. To locate this hidden escape platform, mice had to rely on four distant visual cues placed on each wall of the water maze room. Mice were trained to find the platform for eight trials per day (two non-consecutive blocks of four trials with starting points selected pseudo-randomly) and, once the platform was located, they were allowed to stay on it for 20 s before the next trial started. If a mouse did not find the platform within 60 s, the animal was gently guided to it and a score of 61 s was recorded for that trial. Latencies-to-find-platform were measured in each training session. For testing reference memory, single probe trials were carried out 24 h after the last training session. Mice were released at a random starting positions and were allowed to swim during 60 s in the absence of the platform. All trials were video recorded for later off-line analysis.

Whole-body plethysmography

Respiratory parameters were measured by unrestrained whole-body plethysmography (Data Sciences International) as in Macías et al., 2014. Mice were maintained in a hermetic chamber with controlled normoxic airflow (1.1 l/min 20.5% O_2, 0.5% CO_2, 79% N2) until they were calm. Mice were then exposed to pre-mixed hypoxic air (1.1 l/min) of 16% O2 (and 84% N2) or 10% O_2 (and 90% N2) (BOC Healthcare) for 15 min. Real-time data were recorded and analyzed using Ponemah software (Data Sciences International). Each mouse was monitored throughout the experiment and periods of movements and/or grooming were noted and subsequently removed from the analysis. The transition periods between normoxia and hypoxia (3 min) were also removed from the analysis.

Statistics and data analysis

Statistical analysis was performed using SPSS software. One-way analysis of variance (ANOVA) with Fisher´s least significant difference (LSD) as post hoc comparisons was used to evaluate multiple groups with one independent variable. Multiple groups with two independent variables were compared using two-way ANOVA with LSD as post hoc comparison. Results are presented as means ± SEM.

Supplemental References

Ishii, T., Omura, M., and Mombaerts, P. (2004). Protocols for two- and three-color fluorescent RNA in situ hybridization of the main and accessory olfactory epithelia in mouse. J. Neurocytol. *33*, 657-669.

Paxinos, G., Franklin, K.B. (2001). The Mouse Brain in Stereotaxic Coordinates. Second Edition. Elsevier Academic Press.

Rounds, S.A., Wilde, F.D., and Ritz, G.F. (2013). Dissolved oxygen (ver. 3.0): In National Field Manual for the Collection of Water-Quality Data (U.S. Geological Survey Techniques of Water Resources Investigations), Chapter 6, pp. 1-55.

Schmid, A., Pyrski, M., Biel, M., Leinders-Zufall, T., and Zufall, F. (2010). Grueneberg ganglion neurons are finely tuned cold sensors. J. Neurosci. *30*, 7563-7568.